GALACTIC COSMOCHRONOLOGY

Pagel §10.3.1

- TOPIC now largely MOOT
  - T_{UNIV} from CMB
  - $T_{\star}$'s from Stellar Evolution
  - CHRONOMETERS depend on
    - production ratios
    - history of star formation (prior to isolation of Sun)

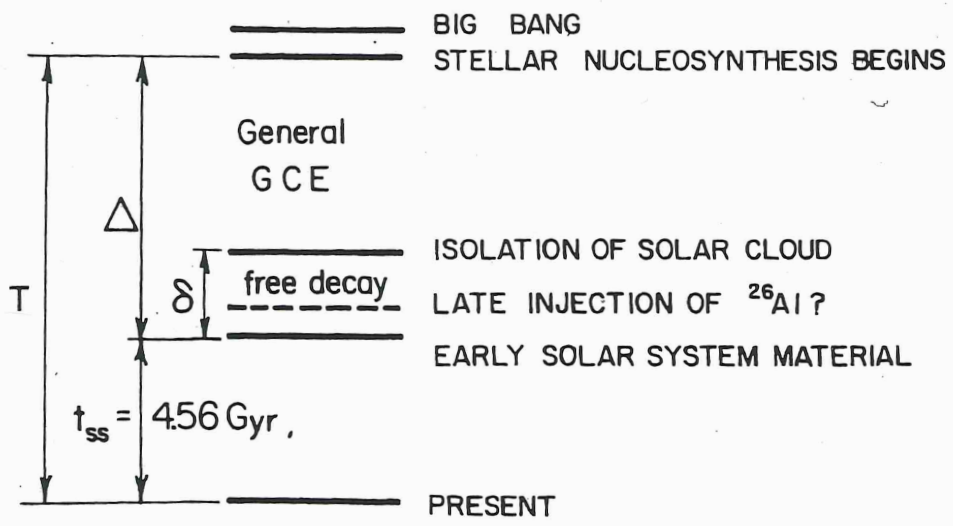

Fig. 10.2. Timescales related to Galactic cosmochronology.

GALACTIC CHRONOMETERS

- SOLAR SYSTEM

  $^{235}U/^{238}U$, $^{232}Th/^{235}U$, $^{244}Pu/^{238}U$

- $T = \Delta + t_{SS} = \Delta + 4.56$ [Gyr]

BUT

a) late spike from a local SN:

$^{129}I \rightarrow$ no ; live ^{26}Al but maybe AGB rather than SN II (?)

b) Free decay, δ . $\delta < 10^7$ yr from short-lived radionuclides

c) $\Delta = \Delta(t)$ for synthesis

MODEL for GALACTIC N' SYNTHESIS

FOWLER (1987)

SPIKE + ongoing production

: S = fraction of stable element from spike

$S = 1$ U-Th → 6.4 Gyr

$S = 0.17 \pm 0.02$
$T = 10 \pm 1.5$ Gyr
} > $^{235}U - ^{238}U$, U - Th

BUT

ALL DEPENDS OF GCE MODEL

"SOLAR-SYSTEM ACTINIDE DATA DO NOT PROVIDE ANY UPPER LIMIT TO THE AGE OF THE GALAXY, NOR DO THEY STRONGLY CONSTRAIN GCE MODELS."

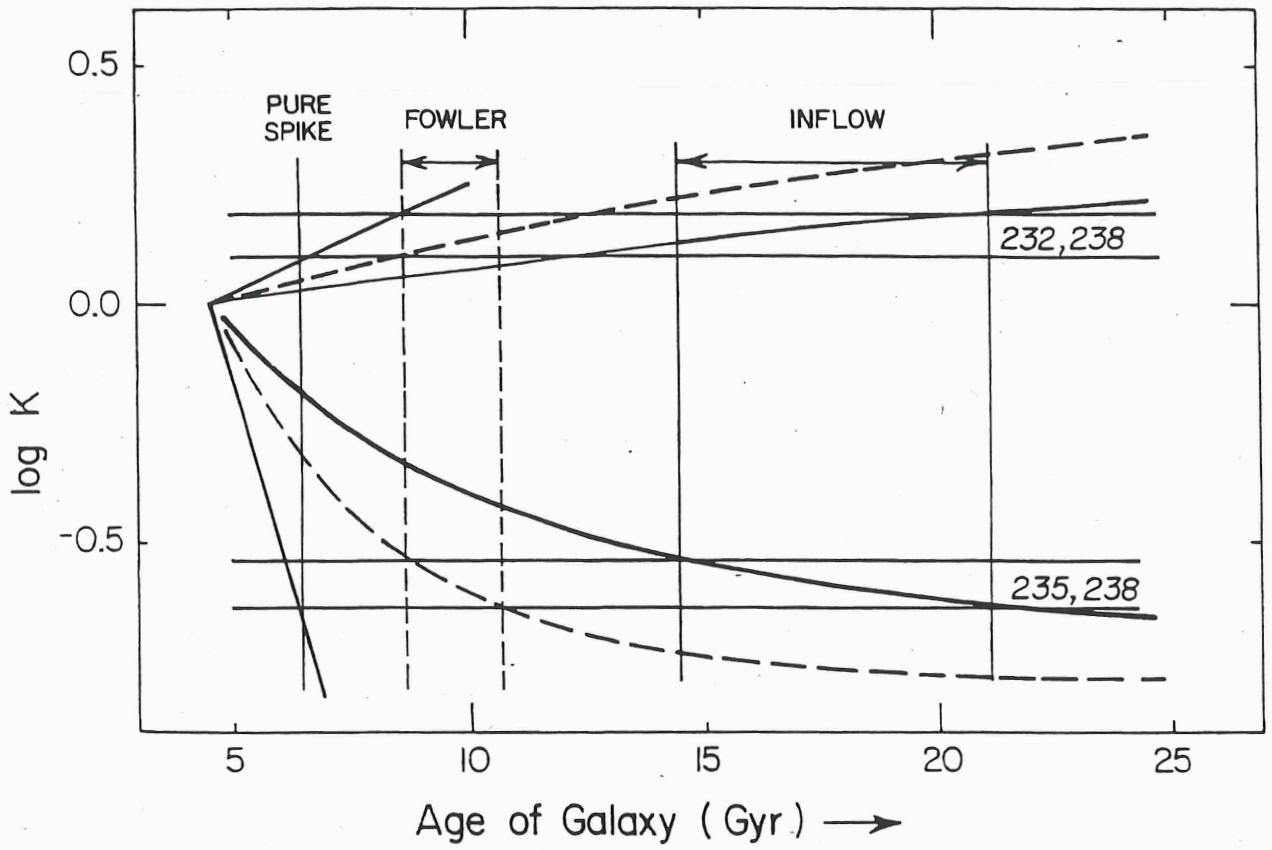

Fig. 10.3. 'Observed' K-ratios (estimated error limits shown by pairs of horizontal lines) and their theoretical variation with the age of the Galaxy according to three models: a pure initial spike (continuous straight lines); Fowler's (1987) model (broken-line curves); and the simple inflow model (continuous curves). After Pagel (1993).

Table 10.2. *Some estimates of K-ratios in the Solar System*

	Meyer & Schramm 1986	Fowler 1987	Cowan *et al.* 1987, 91
p_{235}/p_{238}	$1.5^{+.4}_{-.3}$	$1.34 \pm .19$	1.16
N_{235}/N_{238} [a]	0.310	0.33	0.32
p_{232}/p_{238}	$1.6 \pm .2$	$1.71 \pm .07$	$1.65 \pm .05$
N_{232}/N_{238} [a]	$3.5 \pm .2$	2.30	2.32
p_{244}/p_{238}	0.12 to 1		
N_{244}/N_{238} [a]	$0.005 \pm .001$		
$K_{235,238}$	$0.21 \pm .05$	$0.246 \pm .035$	0.273
$K_{232,238}$	$2.2 \pm .3$	$1.35 \pm .10$	$1.40 \pm .05$
$K_{244,238}$	0.004 to 0.05		

[a] At formation of Solar System.

- STARS

  - LONG-LIVED RADIONUCLIDES
    ^{232}Th & ^{238}U only
    (14 Gyr) (4.5 Gyr)
  - Th IN MANY STARS, even r↑, metal poor
  - U IN JUST ONE OR TWO (^{238}U)

  - MEASURE
    Th/U | stable actinides

  - SET LIMIT TO

$$\Delta' = t_{CMB} - t_{\substack{OLDEST \\ STAR}}$$

BUT NEED TO KNOW Th/U PRODUCTION RATIOS

- SN II vs NS+NS production?

- r-process is stable-r but for all Z?

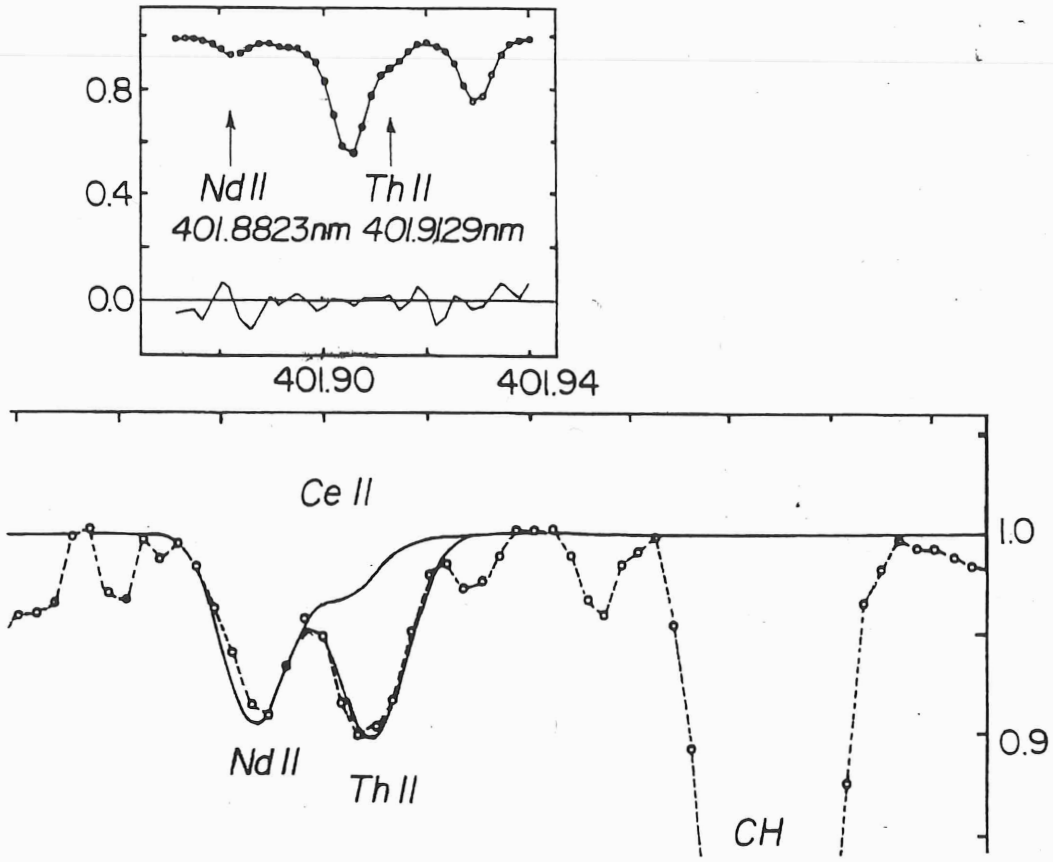

Fig. 10.4. Above: spectrum of the solar-type G-dwarf star HR 509 showing features of Th II and Nd II near λ 4019 Å, after Butcher (1987). Th II is blended with a strong feature due to Fe and Ni, as well as weaker features. The tracing around the zero level shows 10 × the difference between the observed spectrum (dots) and the fitted synthetic spectrum (continuous curve). Reproduced with permission from Macmillan Magazines Ltd. Below: spectrum of the same region in the very metal-poor giant star CS 22892−052 ([Fe/H] $\simeq -3$) with a large relative excess of r-process elements ([r/Fe] = 1.7), adapted from Sneden *et al.* (1996).

EXAMPLES

- HILL et al. 2002 A&A 387 560
  BARBUY et al. 2011 A&A 534 A60
  FREBEL et al. 2007 ApJ 660 L117

- GIANTS vs DWARFS
- HST SPECTRA → actinides

NEED MORE ∪ STARS

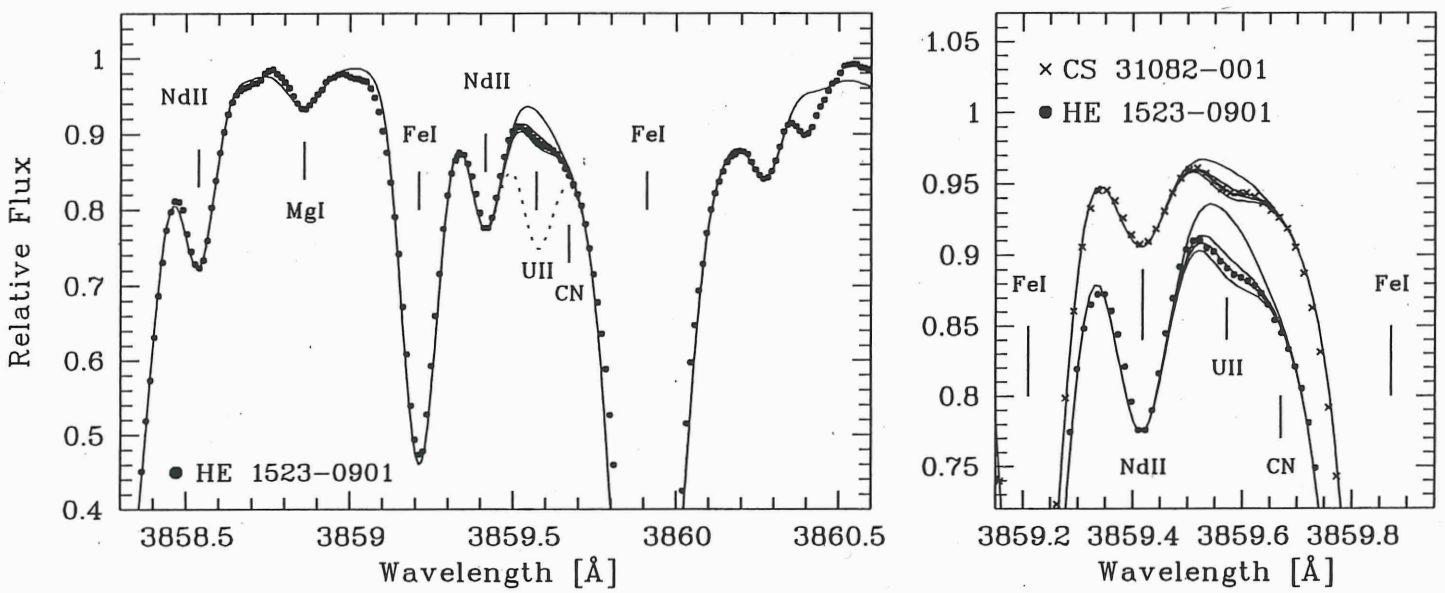

Fig. 7.2: Spectral region around the U II line in HE 1523−0901 (*filled dots*) and CS 31082-001 (*crosses*; right panel only). Overplotted are synthetic spectra with different U abundances of $\log \epsilon(\mathrm{U}) =$ none, −1.96, −2.06, and −2.16 (HE 1523−0901) and $\log \epsilon(\mathrm{U}) =$ none, −2.05, −2.15, and −2.25 (CS 31082-001). The dotted line in the left panel corresponds to a scaled solar r-process U abundance present in the star if no U were decayed. Positions of other features are indicated.

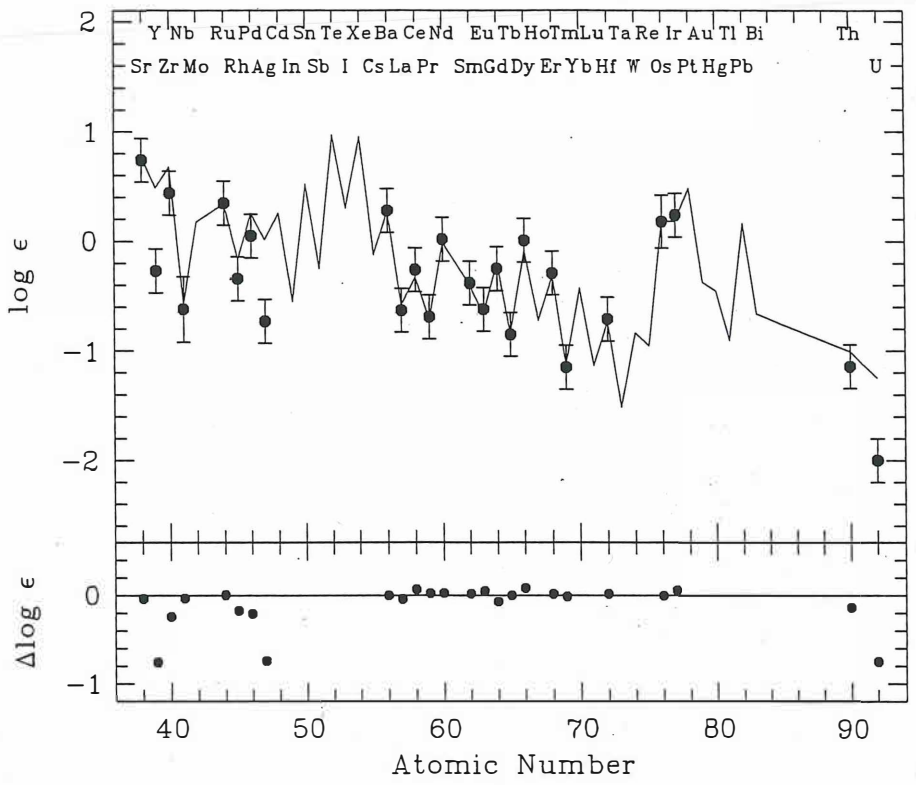

Fig. 7.1: Neutron-capture element abundances of HE 1523−0901 in comparison with those from the solar r-process (Burris et al. 2000) scaled to match the observed elements with $56 \leq Z \leq 69$ (*top panel*). The bottom panel shows the residuals from the abundances of HE 1523−0901 minus the solar r-process values.

Table 7.1. Ages derived from different abundance ratios

X/Y	log(PR)[a]	Ref.	$\log \epsilon(X/Y)_{obs}$	Age (Gyr)	Adopted
Th/Eu	−0.377	1	-0.50 ± 0.10	5.7±4.7	7.8±4.7
Th/Eu	−0.33	2	-0.50 ± 0.10	7.9±4.7	...
Th/Eu	−0.295	3	-0.50 ± 0.10	9.6±4.7	...
Th/Os	−1.15	2	-1.30 ± 0.10	7.0±4.7	7.0±4.7
Th/Ir	−1.18	2	-1.36 ± 0.10	8.4±4.7	11.3±4.7
Th/Ir	−1.058	1	-1.36 ± 0.10	14.1±4.7	...
U/Eu	−0.55	2	-1.44 ± 0.15	13.2±2.2	13.2±2.2
U/Os	−1.37	2	-2.24 ± 0.15	12.9±2.2	12.9±2.2
U/Ir	−1.40	2	-2.30 ± 0.15	13.3±2.2	14.1±2.2
U/Ir	−1.298	3	-2.30 ± 0.15	14.8±2.2	...
U/Th	−0.301	4	-0.94 ± 0.15	13.9±3.3	14.8±3.3
U/Th	−0.29	5	-0.94 ± 0.15	14.1±3.3	...
U/Th	−0.256	3	-0.94 ± 0.15	14.9±3.3	...
U/Th	−0.243	6	-0.94 ± 0.15	15.2±3.3	...
U/Th	−0.22	2	-0.94 ± 0.15	15.7±3.3	...

[a]PR: initial production ratio

Refs. — 1: Sneden et al. (2003), 2: Schatz et al. (2002), 3: Cowan et al. (2002), 4: Goriely & Arnould (2001), 5: Wanajo et al. (2002), 6: Dauphas (2005)

TYPE Ia SN & NUCLEOSYNTHESIS

PAGEL §5.11

ILIADIS §5.5.1

N-S IMPORTANCE

- SOURCE OF Fe-PEAK ELEMENTS
  (DELAYED W.R.T. SN II :
  lower mass, mergers ?)

OTHER IMPORTANCE

- STANDARD CANDLES
  → HUBBLE CONSTANT
  → DARK ENERGY

HISTORY

- ZWICKY : SN I & SN II
- WHEELER SN Ia & SN II / IIb / Ic
- HOYLE + FOWLER
  (1960 ApJ 132 565)

Ia = "ignition of degenerate nuclear fuel in stellar material"

→ r-process in Type I SN !

LIGHT CURVES

v. uniform after Phillips' relation/correction

LOCATION

- PRESENT in ALL GALAXIES incl. ELLIPTICAL
- NOT EXCLUSIVELY IN SPIRAL DISKS but also in SPIRAL HALOS

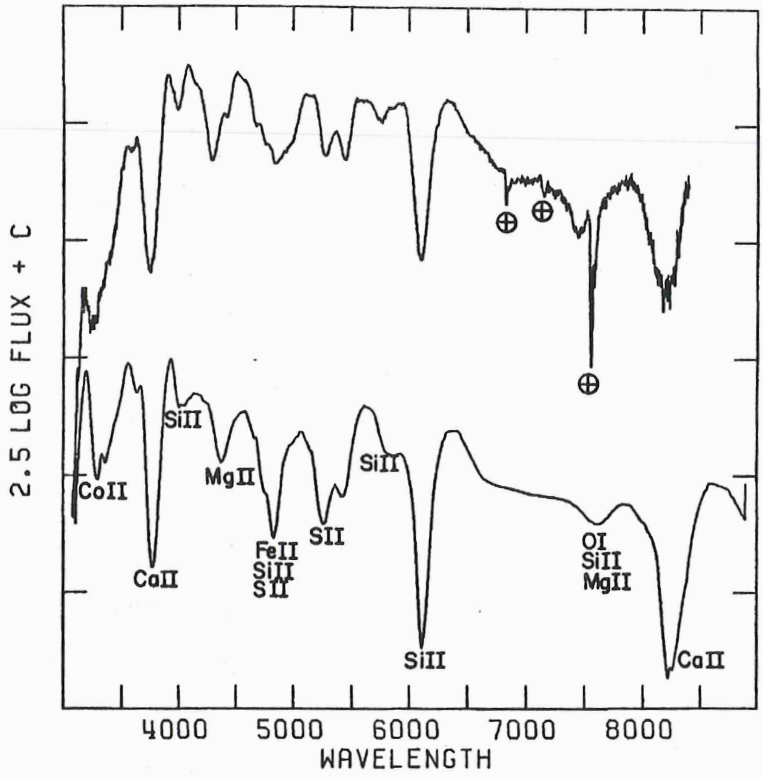

Figure 7 The March 7 (maximum light) spectrum (top) of SN 1981b (Branch et al. 1983) is compared with a synthetic spectrum (below) for deflagration model W7 (Nomoto et al. 1984b). In order to obtain the good agreement shown, it was necessary to mix the composition in Figure 5 external to 0.65 $M_\odot$ ($v \sim 10^4$ km s^{-1}). Terrestrial absorption features in the observed spectrum (circled crosses) are indicated. Figure taken from Branch et al. (1985).

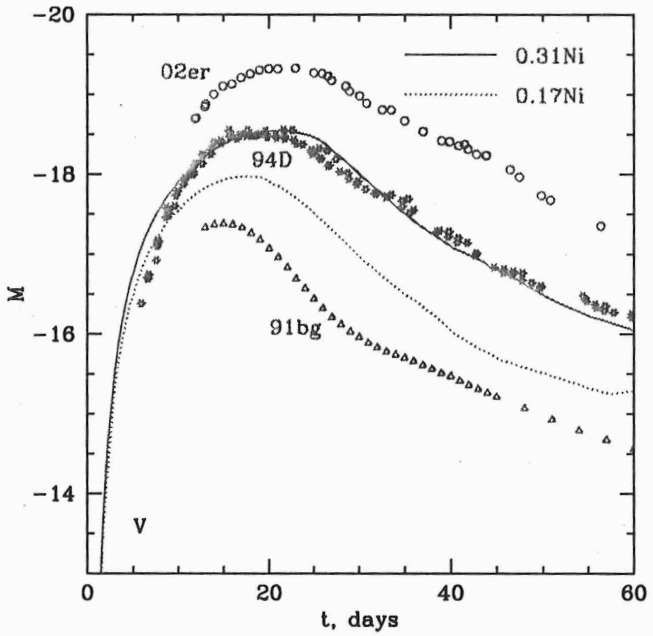

Fig. 3. Theoretical (solid and dashed lines) of two 3D models with different Ni masses in comparison with observed V-band lightcurves. SN 1994D was a 'normal' SN Ia, while SN 2003er and SN 1991bg were bright and faint, respectively (Sorokina and Blinnikov, 2003). Note that the highest Ni-masses we could get until now are around 0.4 $M_{\odot}$.

LIGHT CURVES

- RISE to $L_{pk} \sim 10^{10} L_\odot$
  in ~20 DAYS
- INITIAL STEEP DECLINE
  by ~3 mags in 30 days
- SLOWER DECLINE WITH
  $t \sim 70$ days

SPECTRA

- MAX : Si, Ca, Mg, S & O
  8000 - 30000 km/s
- 14 DAYS Fe II
- 30 DAYS Fe II Fe III, Co II

ENERGY REQUIREMENTS

- KE of EJECTA $\sim 10^{51}$ ergs
- EM emission $\sim 10^{49}$ ergs

BURN 1 $M_\odot$ of C+O to Fe

$\longrightarrow$ 10^{51} ergs

LIGHT CURVE powered by RADIOACTIVE DECAY of ^{56}Ni [principally]

$^{56}Ni \; (\beta^+\nu) \; ^{56}Co \; (\beta^+\nu) \; ^{56}Fe$

$t_{1/2} = 6.1$ days $\quad = 77.2$ days $\quad$ STABLE

Ni mass

$$L_{plc} \sim 2 \times 10^{43} \frac{M_{Ni}}{M_\odot} \text{ ergs}$$

Lplc range $\rightarrow M_{Ni} \sim 0.1$ to $1.0\, M_\odot$

IMMEDIATE PROGENITORS

"DEGENERATE NUCLEAR MATERIAL"

→ NOT THERMOSTATTED AS IN NON-DEGENERATE MATERIAL

- EXPLOSION TRIGGERED BY $m_{WD} \geq m_{CHANDRA}$
- He WD?
  - SINGLE STARS ↛ He WHITE DWARF IN LIFETIME OF GALAXY
  - BINARY STAR → He WD + comp.
  - $m > m_{CH}$ → VERY VIOLENT, TOO ENERGETIC → NO INTERMEDIATE MASS ELEMENTS (Si, S, Ca) but these are common.

DETONATION before m_{CH}

CO WD - see next

ONeMg WD — COLLAPSE THANKS TO ELECTRON CAPTURE ON ^{24}Mg

$^{24}Mg + e^-$ $\quad \rho_{crit} \sim 10^{9.6}$

$^{20}Ne + e^-$ $\quad \sim 10^{9.8}$

$$^{24}Mg + e^- \rightarrow {}^{24}Na + \nu_e$$

$$^{24}Na \rightarrow {}^{24}Mg + e^- + \bar{\nu}_e$$

→ STRONG NEUTRINO cooling

URCA PROCESS

In degenerate electron gas, the e^- at the Fermi energy may have sufficient energy to convert ^{24}Mg to ^{24}Na

(See Arnett, p168)

CO WD → $\gtrsim M_{ch}$

ACCRETION from a COMPANION

- WD + main sequence
- WD + red giant

} not normal star

MERGER of PAIR of WDs

- DOUBLE DEGENERATE

HOMOGENEITY of SN Ia ?

→ SIMILAR ACCRETION/MERGERS

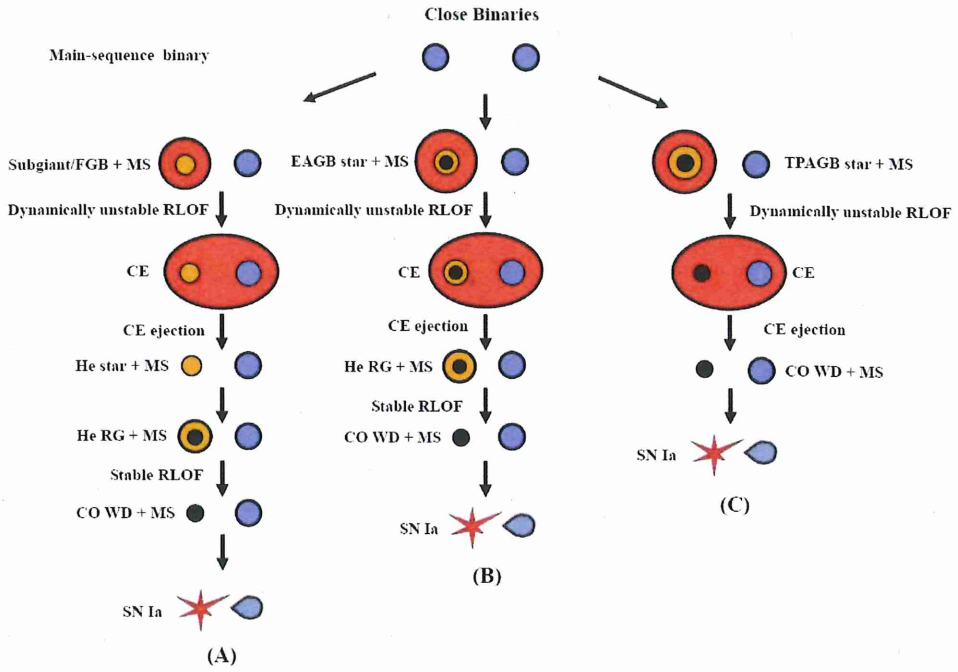

Figure 1: Binary evolutionary scenarios of the WD + MS channel for producing SNe Ia.

Wang & Han 2012 New Astr. 56, 122

ROUTES for CLOSE BINARY

→ CO_{WD} + MS

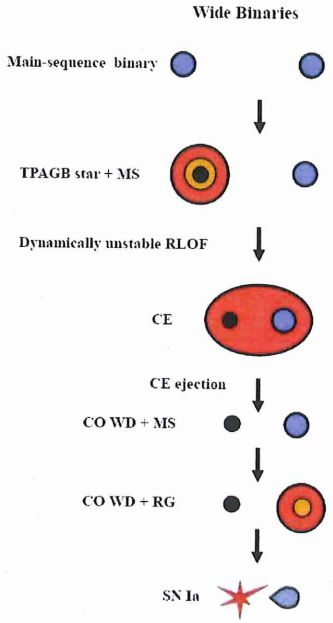

Figure 2: Similar to Fig. 1, but for the WD + RG channel.

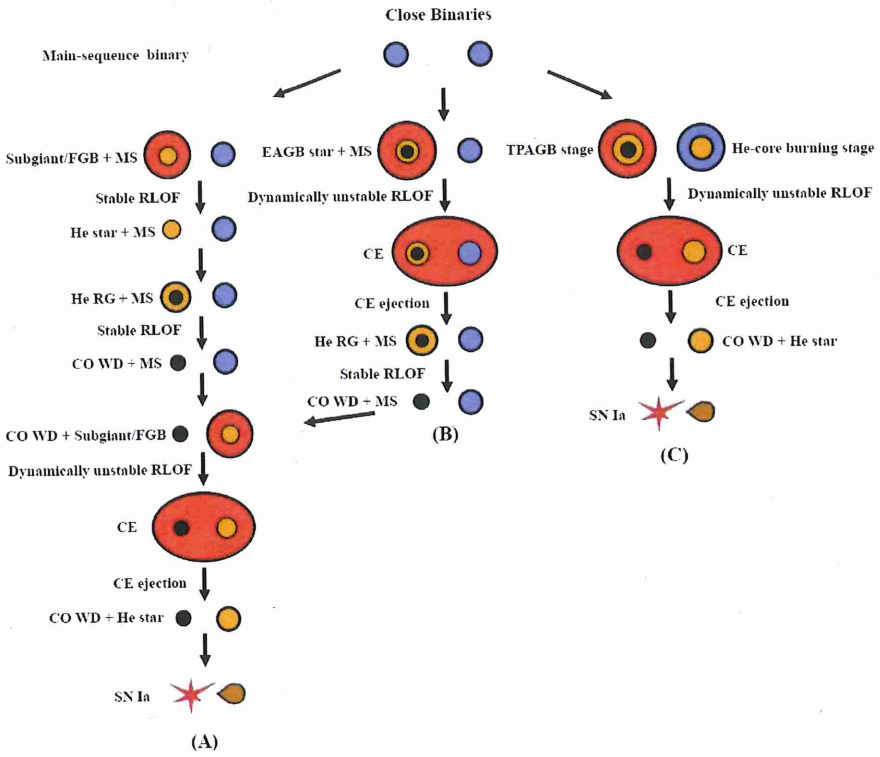

Figure 3: Similar to Fig. 1, but for the WD + He channel.

→ CO_{WD} + He STAR

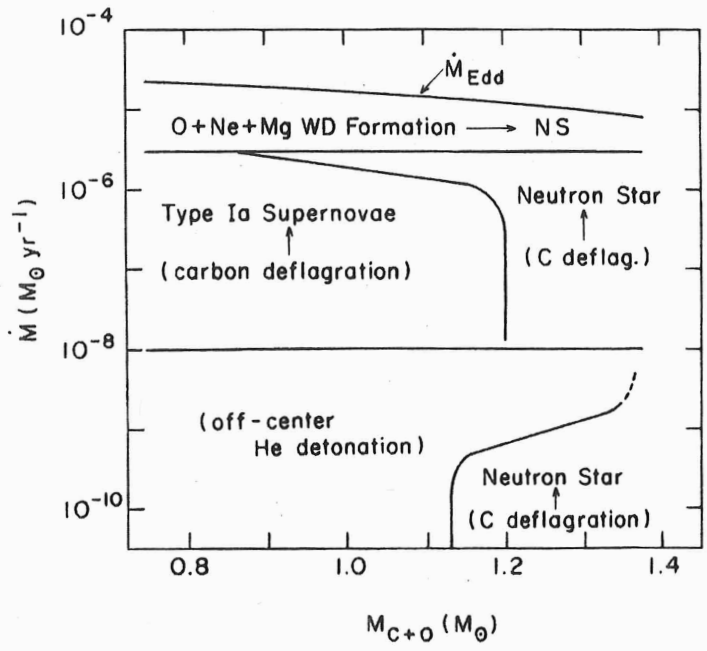

Fig. 5.23. Possible outcomes of accretion on to a CO white dwarf, according to its mass and accretion rate. $\dot{M}_{Edd}$ is the critical (Eddington) rate above which radiation pressure drives material out. After Nomoto and Kondo (1991). Courtesy Ken-ichi Nomoto.

$\dot{m} < 10^{-9} M_\odot/yr$ H-rich → Novae
$\propto m_{WD} \sim$ const.

He-rich → No nova
(T too low for)
He burning
$\propto M_{WD}$ grows

DOUBLE DEGENERATES

- frequency ? - std. candle ?

ACCRETION SCENARIO : $M \sim M_{CH}$

- $m_{CO} \leq 1.1 M_\odot$ for normal WD
- NOT EASY to ACCRETE $0.3 M_\odot$

The $\dot{m}$ is KEY to get ACCRETION, BURN H to He-CO AND AVOID EJECTION (NOVAE)

ACCRETION SCENARIO - $M < M_{CH}$
(SUB-CHANDRA.)

He ACCRETION ONTO LOW MASS C-O WD

- He BURNS AT SURFACE OF C-O WD

→ DOUBLE SHOCK

- OUTWARD BURNING OF He to ^{56}Ni
- INWARD BURNING OF CARBON

→ LESS ^{56}Ni → FAINTER SN Ia than M_{CH} SN Ia

→ MAY HELP WITH NUCLEOSYNTHESIS (p NUCLEI, ^{44}Ca)

→ BUT MAY NEED TIGHT LIMIT ON $\dot{M}$

$m \gtrsim m_{ch}$: CO WD

IGNITION

- DEFLAGRATION
  burning front/flame grows by conduction → SUBSONIC
- DETONATION
  burning front driven by a shock → SUPERSONIC

IGNITION REGIMES

- PROMPT DETONATION
  - BURNING INTO DENSE LAYERS
  - C-O ⇒ Fe GROUP WITH LITTLE INTER. ELEMENTS
  - DOES NOT FIT TYPICAL SPECTRUM
- DEFLAGRATION
  - PRODUCES INTER. ELEMENTS AS LAYERS EXPAND AHEAD OF FLAME
  - SOME UNBURNT C-O ?

DELAYED DETONATION

- INITIAL DEFLAGRATION
  → EXPANSION → DETONATION

- PRODUCES INTER. ELEMENTS
  & ACCOUNTS FOR LIGHT CURVE
  & EXPANSION VELOCITIES

- DEFLAGRATION → DETONATION ?

See Maeda et al. 2010 ApJ 712 624

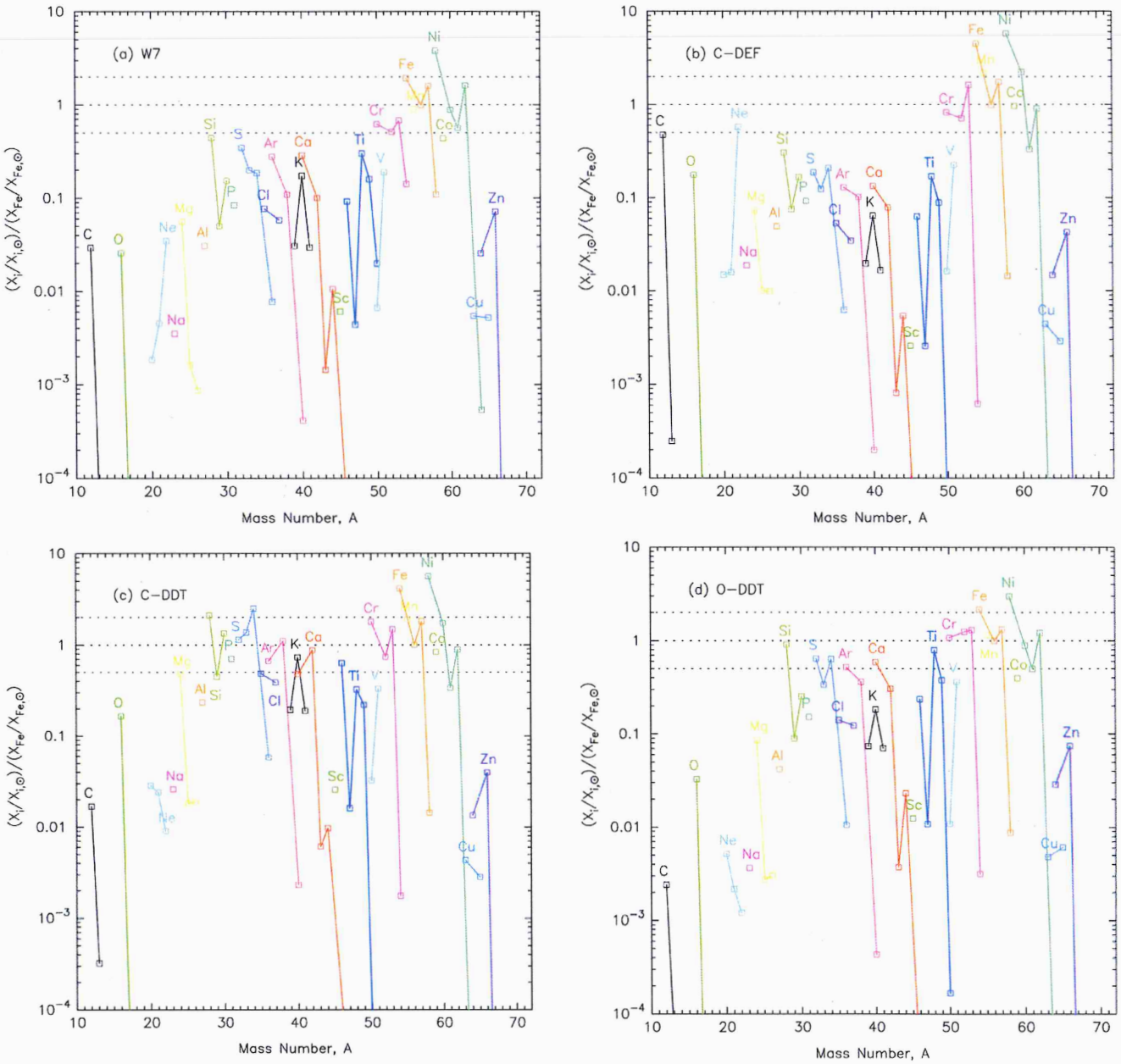

Figure 13. Isotopic yields integrated within the whole ejecta (after radioactive decays). The mass fraction is shown relative to the solar value and normalized by ^{56}Fe. (A color version of this figure is available in the online journal.)

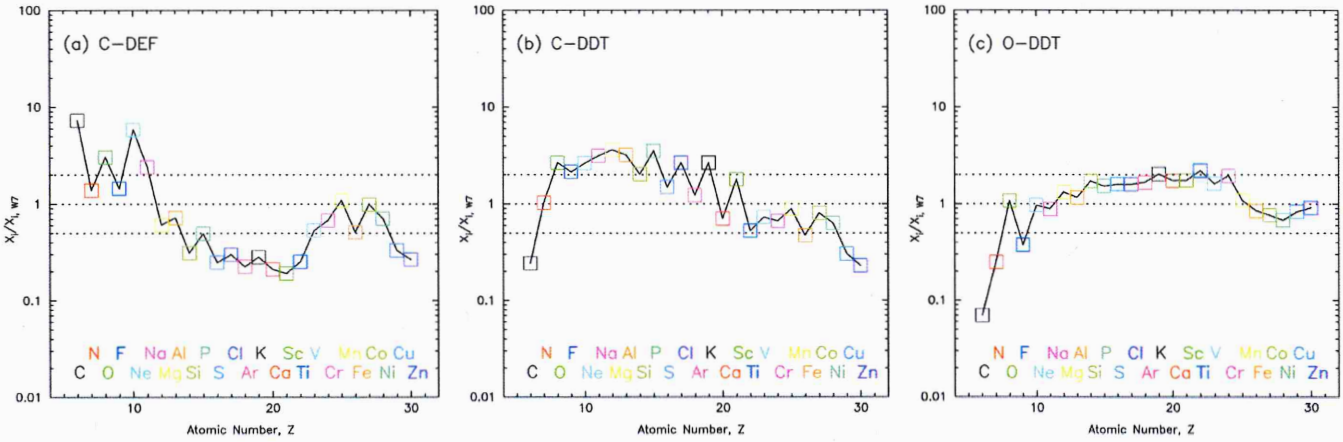

Figure 14. Ratios of integrated element yields to the W7 model yields.
(A color version of this figure is available in the online journal.)

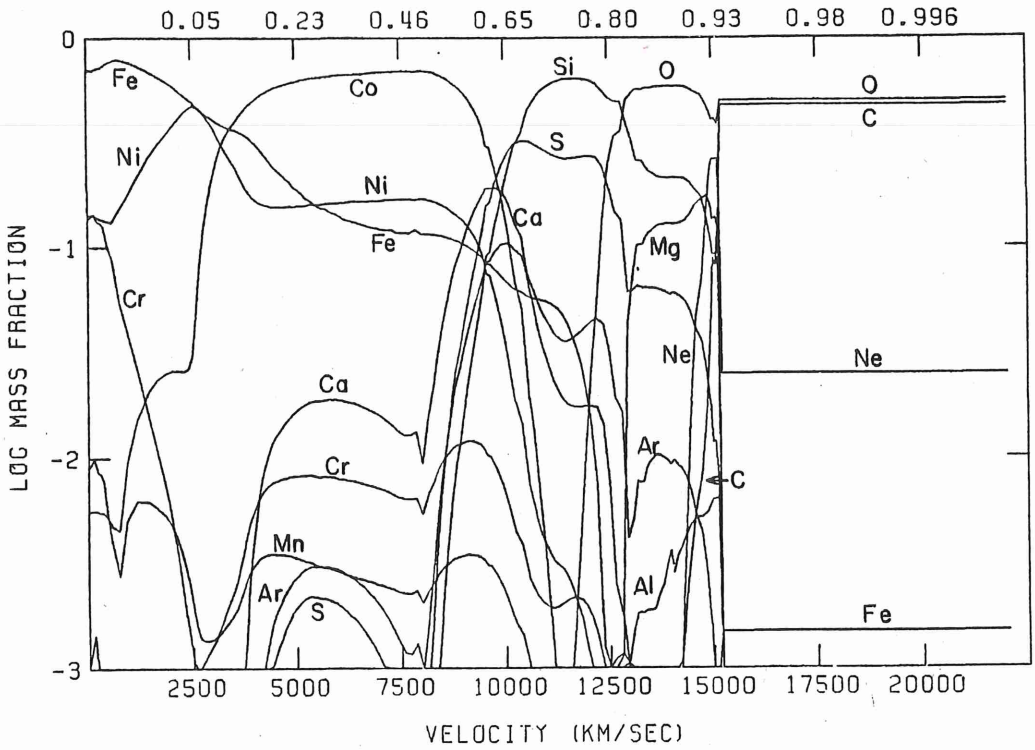

Figure 5 Composition of a carbon deflagration model for Type I supernovae (Model W7 of Nomoto et al. 1984b) as a function of interior mass in solar masses (top of figure) and asymptotic expansion velocity (bottom of figure). The composition is sampled at a time near maximum light (15 days). All of the cobalt shown will later decay to ^{56}Fe. Figure taken from Branch et al. (1985).

NSE Incomplete Si-burning | C/Ne burning | unburnt

Incomplete O-burning

EXAMPLE OF CARBON DEFLAGRATION SN Ia (W7)

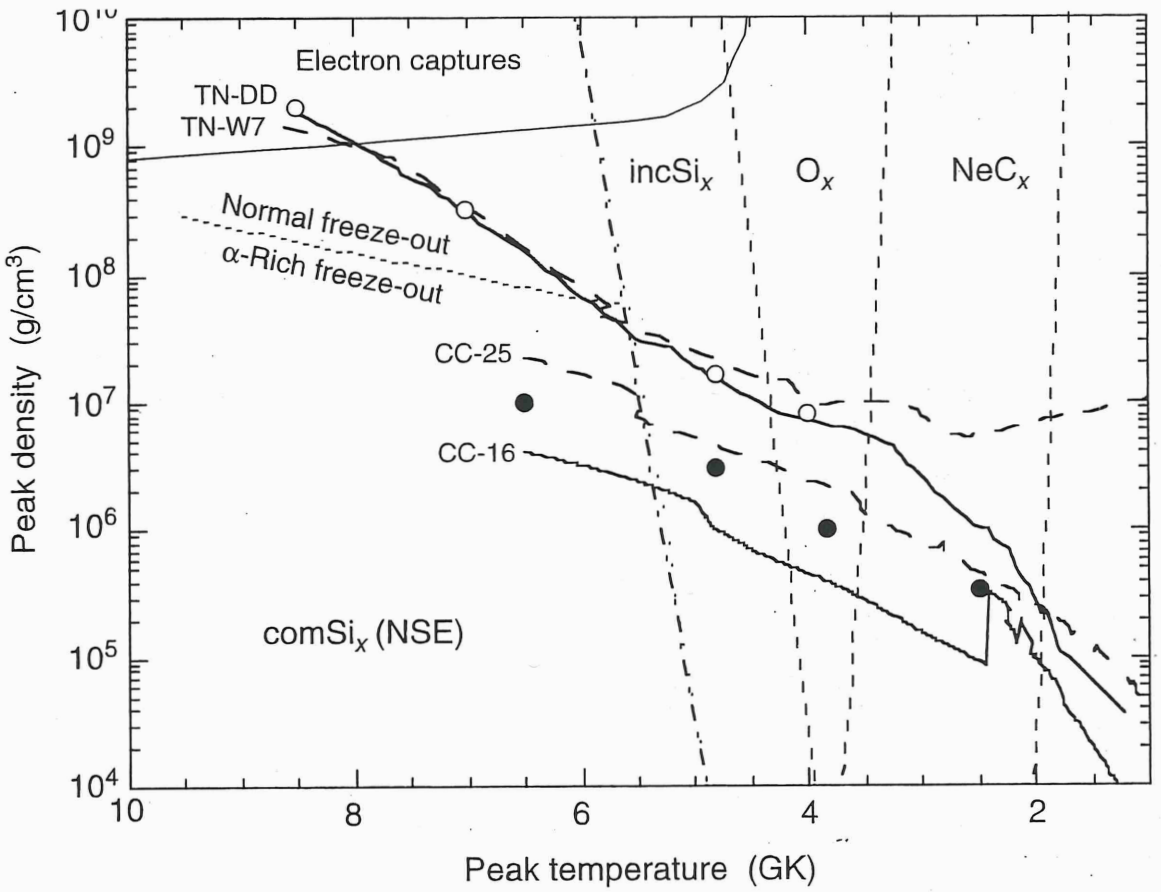

Figure 5.42 Peak temperatures and peak densities attained in different mass zones during the outward propagation of burning fronts in supernova explosion models. The two lower tracks are from core-collapse (type II, Ib, Ic) supernova models (CC-16: Young *et al.*, 2006; CC-25: Limongi and Chieffi, 2003), while the two upper tracks are from thermonuclear (type Ia) supernova models (TN-W7: Nomoto, Thielemann, and Yokoi, 1984; TN-DD: Bravo and Martínez-Pinedo, 2012). Regions of predominant nucleosynthesis processes are indicated: complete silicon burning ("comSi$_x$ (NSE)", entire region to the left of dashed-dotted line); normal freeze-out (above dotted line); α-rich freeze-out (below dotted line); incomplete silicon burning ("incSi$_x$"), explosive oxygen burning ("O$_x$"), and explosive neon-carbon burning ("NeC$_x$"). The boundaries between the different regions depend on the explosion time scale and are only approximate. The gray shaded area at the top left indicates the region where electron captures change the neutron excess significantly during the explosion (Section 5.5.1). The full and open circles mark peak temperature and density conditions adopted for the reaction network calculations discussed in the text.

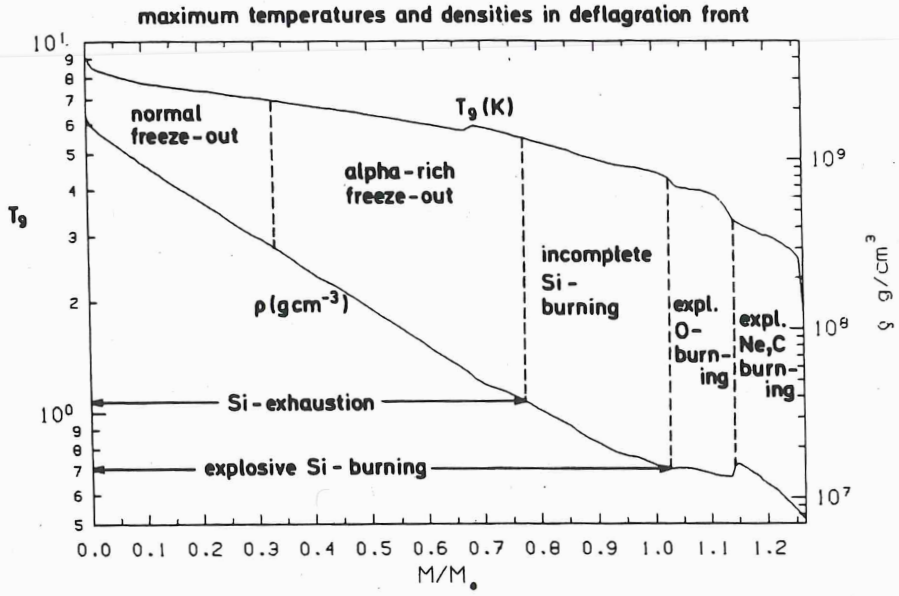

Fig. 5.24. Maximum temperatures and densities calculated for an outward propagating deflagration front in a model (model W7) of an SN Ia explosion from accretion on to a CO white dwarf with initial mass 1 $M_\odot$ at a rate of 4×10^{-8} $M_\odot$ yr^{-1}. Zones of different burning conditions are indicated. After Thielemann, Nomoto and Yokoi (1986). Courtesy Ken-ichi Nomoto.

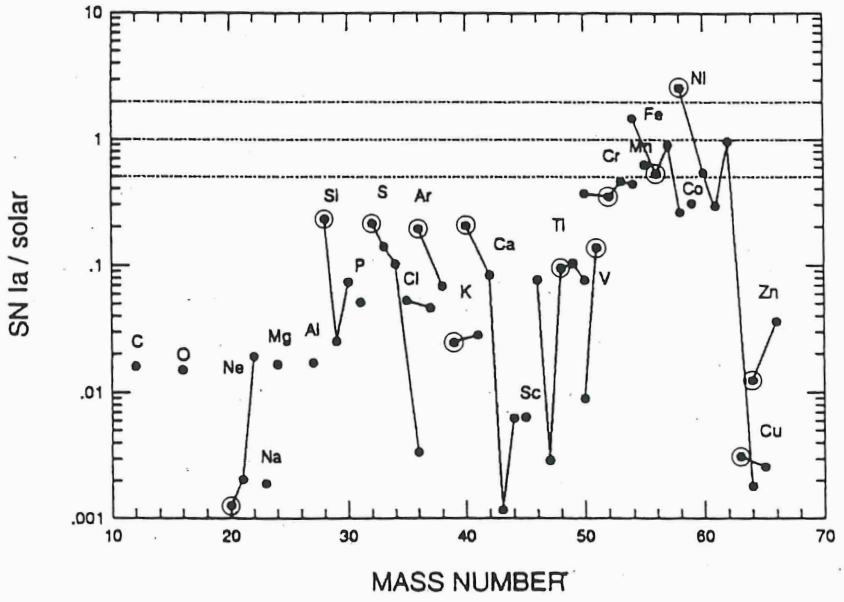

Fig. 5.25. Nucleosynthetic outcome (after radioactive decay) of model W7 for Type Ia supernovae (Nomoto, Thielemann & Yokoi 1984, and Thielemann, Nomoto & Yokoi 1986), compared to Solar-System abundances. Dominant isotopes of multi-isotope elements are circled. Adapted from Tsujimoto (1993).

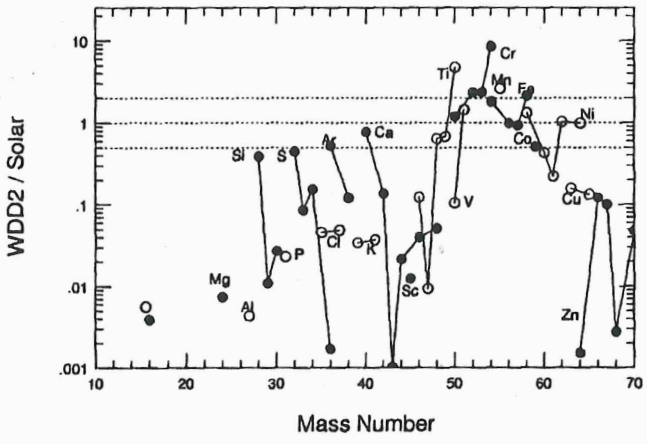

Figure 5. The ratios of integrated abundances of the delayed detonation model WDD2 after decay of unstable nuclei, normalized to ^{56}Fe, relative to solar abundances.

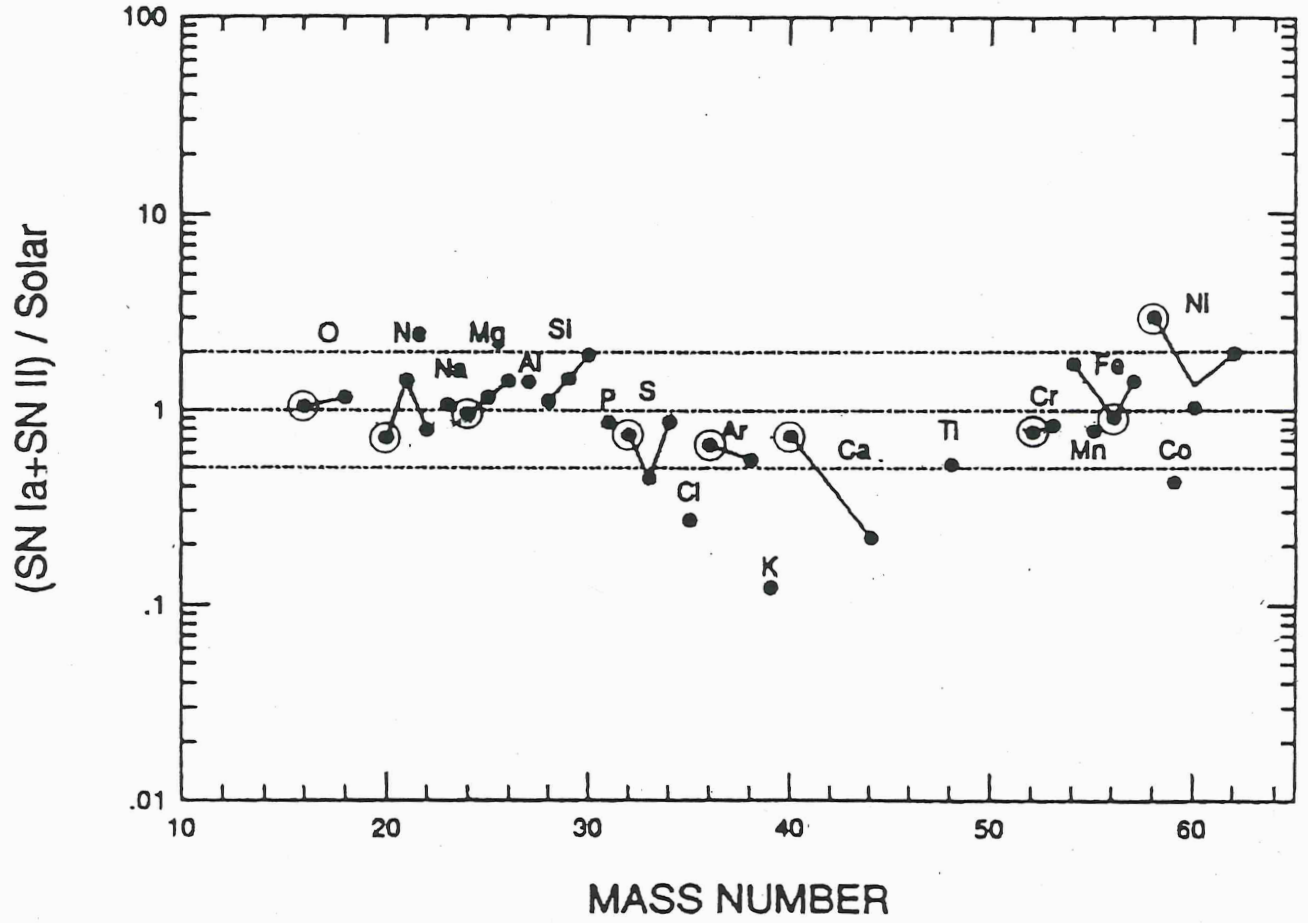

Fig. 5.26. Nucleosynthesis products from SN Ia (Fig. 5.25) and SN II (Fig. 5.12) combined in a ratio of 1:10, compared to Solar-System abundances. (A slightly higher ratio of 1:7 gives optimal fit to elemental, as opposed to individual nuclidic abundances.) Dominant isotopes of multi-isotope elements are circled. Adapted from Tsujimoto (1993).

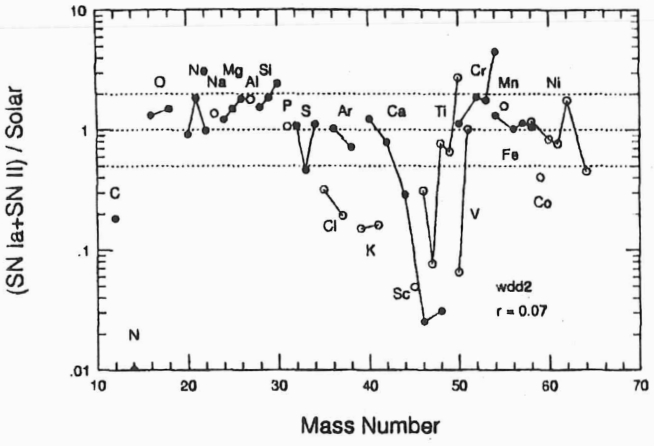

Figure 6. Solar abundance pattern based on synthesized heavy elements from a composite of Type Ia and Type II supernova explosions with the most probable ratio of r. Relative abundances of synthesized heavy elements and their isotopes normalized to the corresponding solar abundances are shown by circles. Here WDD2 is adopted for the Type Ia supernova model.

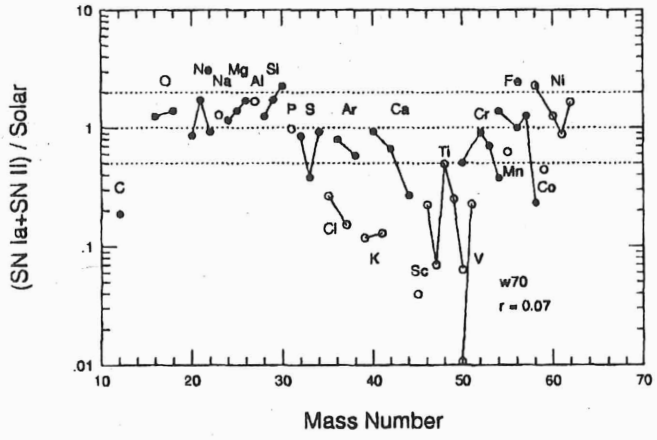

Figure 7. Same as Figure 6 but for W70 as an SN Ia model.

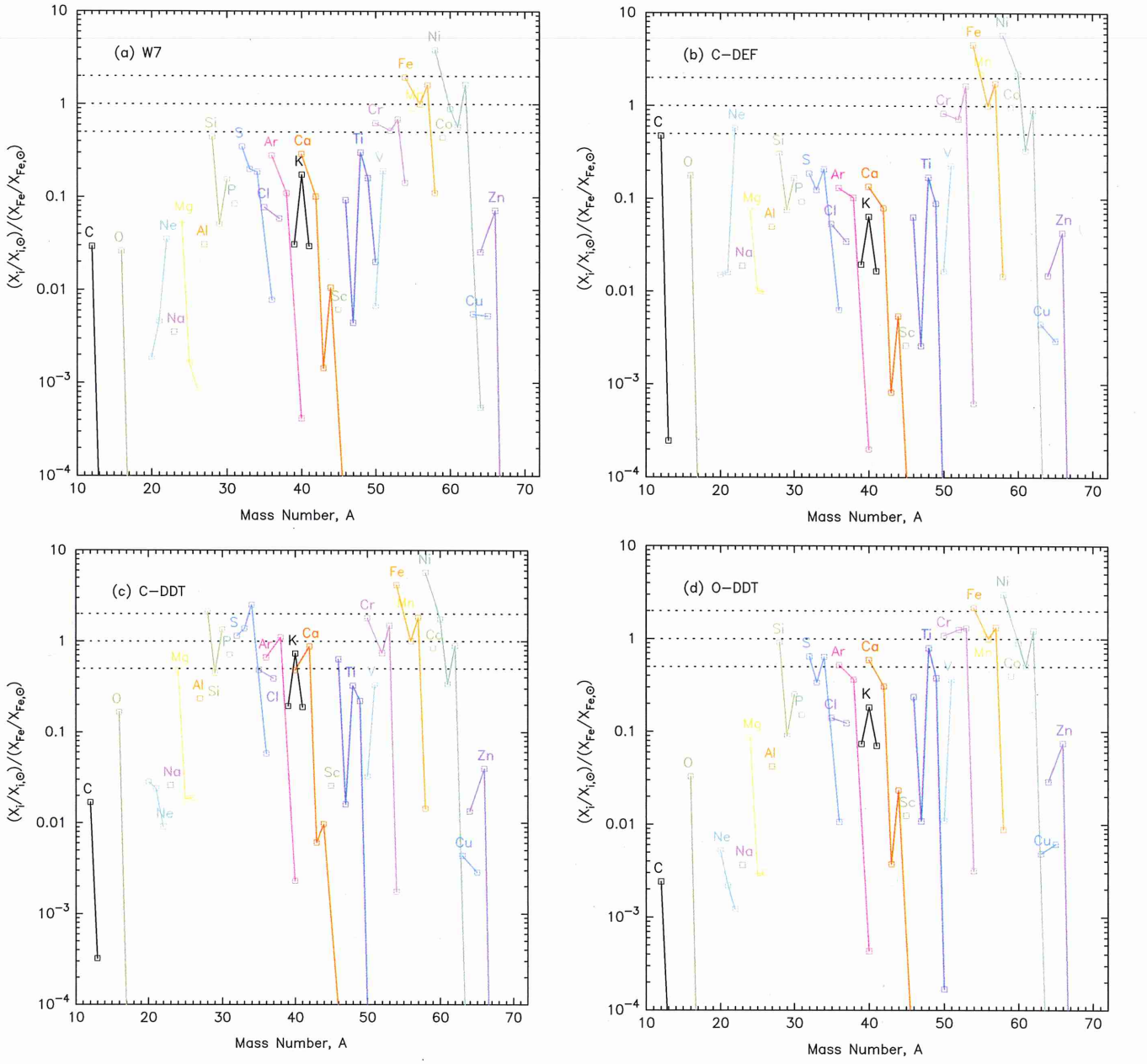

Figure 13. Isotopic yields integrated within the whole ejecta (after radioactive decays). The mass fraction is shown relative to the solar value and normalized by ^{56}Fe. (A color version of this figure is available in the online journal.)

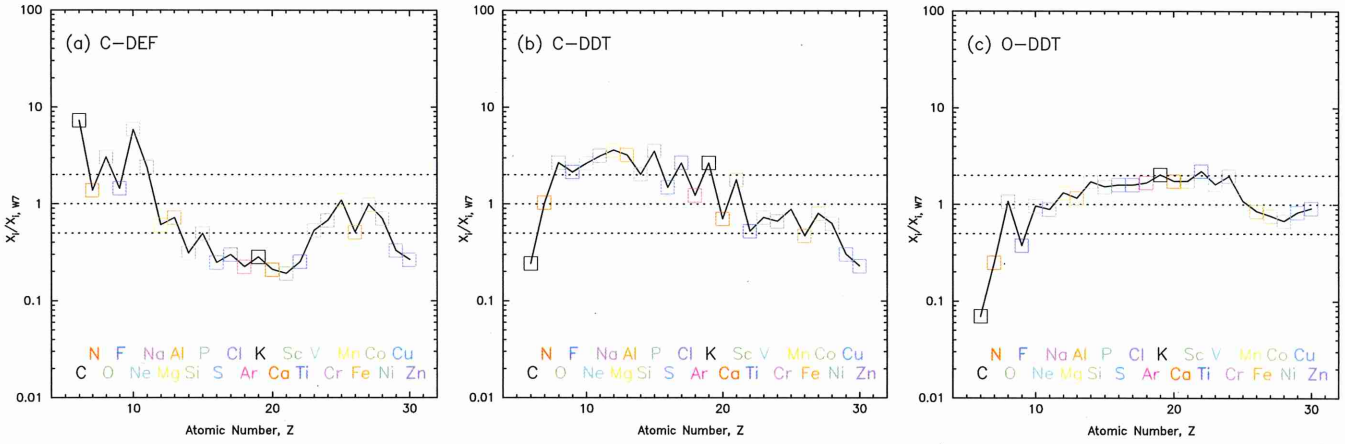

Figure 14. Ratios of integrated element yields to the W7 model yields. (A color version of this figure is available in the online journal.)

GALACTIC CONTEXT

	SN Ia	SN Ib/c	SN II
RATE (per 100 yr)	0.2 - 0.3	0.65	3.3
M_{Fe}	0.6	0.3	$0.07 M_\odot$

MILKY WAY

Now ~50% of Fe from SN Ia

but this was delayed because Ia's take time pre-SN